

Cable Breaking Probability Analysis of Cable-Stayed Bridge Subjected to the Environmental Corrosion and Fatigue Load

HE Min¹, CHEN Zhaohui² and GU Hong³

¹School of Civil Engineering, Chongqing University, Chongqing, 400045, China. hemin.cqu@foxmail.com

²School of Civil Engineering, Chongqing University, Chongqing, 400045, China. zhaohuic@cqu.edu.cn (corresponding author)

³School of Civil Engineering, Chongqing University, Chongqing, 400045, China. 925490577@qq.com

Abstract: The collapse of the cable-stayed bridge caused by the break of cables due to the environmental erosion often happened especially for the aged bridge. During the service life, the cable strength would be decreased due to the interaction of the environmental corrosion and the fatigue stress of load to result in the breaking of the cables. Therefore, the investigation on the time-varying degradation of the strength of the corroded cable in service life and the corresponding impacts on the reliability of cables are crucial to the maintenance of the cable-stayed bridge. Based on the corrosion characteristics of cables and by the application of the fatigue fracture model, the degradation model of the cable strength under the interaction of environmental corrosion and the load stress is proposed, in which the pitting corrosion with the effects of load stress as well as the fatigue cracking are considered. A cable-stayed bridge in Chongqing, China, is chosen for numerical simulation. The analysis shows that the strength of the corrosion cable follows the lognormal distribution with the mean value decreases and the variances increase with time. The reliabilities of the cables under the corrosion and fatigue are also predicted. It is shown that the load stresses have important impact on either the strengths or the reliabilities of the cables. The reliabilities of the back cables and the long cables at the middle of the bridge that have larger stress decreased more rapidly than the cables near the tower.

Key words: cable-stayed bridge, cable corrosion, fracture toughness, fatigue, reliability.

1. Introduction

Cable-stayed bridge has become the most competitive type in long-span bridge because of its excellent mechanical properties, economic in construction and lightness in shape (Chen 2006). During the service life of the bridge, the cables are subject to the dead load, such as the weights of the bridge and the vehicle, and the living load such as the wind load and vehicle load et al. In addition, they are prone to the environmental corrosion which would result in the reduction of cable strength with the interaction of fatigues stresses of living load (Wang et al. 2007).

The corrosion characteristics of the cable has drawn attentions by engineers and researchers in recent years. According to Xu (Xu 2006), in general, the corrosion of the cable wires can be divided into six stages, including the intact stage, the zinc coat corrosion stage, general corrosion stage, pitting corrosion stage, corrosion fatigue coupling stage and the stress dominant corrosion stage, while the corrosion rate is varied in different stage and is speed up from pitting stage. Furuya and Kitagawa investigated on several corrosion cases of the main cables of suspension bridges in Japan (Furuya et al. 2000), and proposed that the corrosion of galvanized cable wires usually started at the surface of the cable and expanded to the core. The corrosion of the outer wires was more severe than the inner ones. These corrosion cases are coincided with the investigations on the cable corrosion of Shimen Bridge in Chongqing, China by Chen, Xu etc. (Xu 2006). The results showed that the corrosion of cable wires decreased exponentially with the distance of the wire to the damaged cable sheath in both the radial direction and the circular direction of the cross-section of the cable. Hopwood and Haven (Hopwood and Haven 1984) divided the corrosion of the wire into four grades respected to different critical strength. Mahmoud

(Mahmoud 2007) proposed the strength model of cable wire with corrosion cracks by taking into account the net section and the fracture toughness of the corroded wire. Xu (Xu et al. 2008) used Monte-Carlo simulation method to evaluate the failure probability of the cable according to the critical number of the damaged wires based on the attenuation of the wire strength. However, in these research works, the varying of the degradation rate with corrosion process, especially the acceleration of the corrosion in the last stages, is ignored that would underestimated the damage risk of the corrosion cable.

In addition to the effects of the wire corrosion to the damage of the cable, the reliability of the bridge system due to the deterioration of the cable strength are also studied. Bruneau (Bruneau 1992) applied the plastic mechanism theory for the system reliability analysis of the medium-span cable-stayed bridge and proposed 14 critical failure modes of the bridge. For each failure mode, the simplified linear safety function was present and the second-order moment method was used to calculate the failure probability. Li (Li et al. 2010) used stochastic finite element method to calculate the reliability indexes of the cables, main tower and girder of the cable-stayed bridge. The results showed that the failure probabilities of the cables are significantly higher than those of the main tower and the girder.

It can be seen that the damage of the cables subjected to environmental erosion are critical to the reliability of cable-stayed bridge. For the bridge in service, the corrosion of the cable would be aggravated by the load stress. Therefore, by taking into account the degradation process of cable strength under the interaction of corrosion and stress, the failure probability analysis of the cables of the bridge are important to the service life prediction of the bridge. Herein, the degradation characteristics of the cable strength with time under the interaction of corrosion and fatigue are analyzed by the

application of fracture toughness strength theory. The variation of the cable reliabilities with time and locations of the bridge are also investigated.

2. Deterioration Model of Cable Strength

As mentioned before, the corrosion of the cable in the natural environment is started with the aging and cracking of the sheath and followed by the zinc coat corrosion. Once the zinc coat was exhausted, the cable wires began to corrode. The corrosion of the cable wires will be speeded up by the stress of living load to result in pitting corrosion and the cable would become brittle by the interaction of corrosion and stress till the stress reaching its bearing capacity to make the cable break. In the following section, the degradation characteristics of cable stresses with time are discussed.

2.1 Corrosion of cable wires

2.1.1 The pitting corrosion of wires

The corrosion of wires become severe when pitting corrosion appears. For simplification, the shape of corrode spot can be assumed as hemispheric, with the corrosion expanding rate followed the Faraday's formula (Xu et al. 2003) (Li et al. 2004)

$$\frac{dV}{dt} = \frac{MI_{po}}{nF\rho} \exp\left(-\frac{\Delta H}{RT}\right) \quad (1)$$

in which the volume of the corrode spot is as follows

$$V = \frac{1}{2} \times \frac{4}{3} \pi a^3 \quad (2)$$

Hence

$$\frac{dV}{dt} = 2\pi a^2 \frac{da}{dt} \quad (3)$$

where a is the radius of the corrode spot, $M=55.85$ g/mol, is the molar mass of iron. n is the atomic valence of iron element, $n=3$. F is the Faraday constant, as 96514C/mol. $\rho = 7.8 \times 10^6$ g/m³, is the density of iron; R is the ventilation coefficient, as 8.314J/mol.K; T is the absolute temperature of the external environment. See, the annual average temperature in Chongqing is 18°C, that is $T=291$ K. ΔH is the activation energy of redox reaction between iron and oxygen, $\Delta H = 59.7$ kJ/mol; I_{po} is pitting process coefficient. According to Xun's statistics, I_{po} is 80.79c/s (Xu et al. 2003).

Load stress can not only destroy the passivation oxide film on the surface of the wire, but also prevent the re-passivation of corrosion pitting and accelerate the corrosion rate (Ebara 2007). Considering the effect of stress on pitting corrosion, Sriraman and Pidaparti (Sriraman and Pidaparti 2010) modified the corrosion model by introducing the stress factors as follows

$$\frac{dV}{dt} = \frac{MI_{po}}{nF\rho} \exp\left(-\frac{\Delta H}{RT}\right) C^{3\sigma} \quad (4)$$

where C is the stress factor, and σ is the stress of the wire.

By substituting Eq. (3) into Eq. (4), the radius of the corrode spot under stress is expressed by integration as follows

$$a = [a_0^3 + \frac{MI_{po}}{2\pi nF\rho} \exp\left(-\frac{\Delta H}{RT}\right) C^{3\sigma} t]^{\frac{1}{3}} \quad (5)$$

where $a_0=1.5\mu\text{m}$ for this case. (Xu et al. 2003)

2.1.2 The cracking of wires under interaction of stress and corrosion

With the developing of pitting corrosion, the wires would crack under the interaction of fatigue and corrosion. When the propagation of fatigue crack exceeds the expansion of pitting corrosion, the degradation of the wires capacities is dominated by cracking. Wang (Wang 1998) proposed the Corrosion Fatigue Cracking Propagation Model (CFC in simple) based on the modified static fracture model of fatigue cracking, in which the propagation rate of crack is simulated as follows

$$\frac{da_r}{dN} = \frac{k}{2\pi\sigma_{FF}} (\Delta K - \Delta K_{thcf})^2 \quad (6)$$

where, k is the environment constant, as 1.585; σ_{FF} is the critical fracture stress at the crack tip. ΔK_{thcf} is the threshold of the corrosion fatigue crack, to be 5.54-3.43 R for the stress ratio R according to experimental statistics (Llorca and Sanchez-Galvez 1987), and ΔK , $\Delta K = K_{max} - K_{min}$, is the amplitude of stress intensity factor at the crack tip. In the present paper, the gravity load, train load and wind load on cable-stayed bridges are considered. Thus, K_{max} and K_{min} are the stress intensity factor at the crack tip to the combination of dead load and living load and to the dead load only respectively.

Therefore, the fatigue crack depth with time t can be predicted as

$$a_r = a_c + \frac{k(\Delta K - \Delta K_{thcf})^2 ft}{2\pi\sigma_{FF}^2} \quad (7)$$

where a_c is the critic radius of corrode spot to the start of cracking (Xu et al. 2003). a_c is expressed as follows

$$a_c = \pi \left(\frac{\Delta K_{thcf}}{2.2K_I \Delta \sigma} \right)^2 \quad (8)$$

2.2 Corrosion distribution at the cable cross section

The investigation on the cable corrosion of a cable-stayed bridge in Chongqing by Chen etc. (Xu 2006) showed that the corrosion rate is decreased from outer to inner of the cable and with the distance to the damaged sheath, as shown in Fig.1. Define the relative corrosion rate R as follows

$$R = (d_0 - d_{min}) / (d_0 - d_{min,0}) \quad (9)$$

where, d_0 is the nominal diameter of cable wire; d_{min} and $d_{min,0}$ are the minimum diameter of the wire and the minimum reference diameter of the wire at the broken

sheath respectively. The minimum diameter of wire d_{\min} is

$$d_{\min} = (1 - R)d_0 + R \cdot d_{\min,0} \quad (10)$$

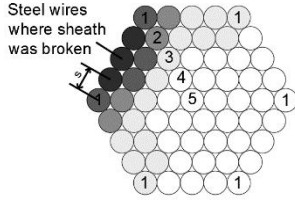


Figure 1. The distribution of corrosion at the cable cross section

2.3 Bearing capacity of the corrosion cables

The cables are mainly subjected to tensile stress so that the corrosion wire could be regarded as an axially stretched rod with unilateral Type I crack, or tensile crack. Based on the theory of linear elastic fracture mechanics, once the stress intensity factor K_I at the crack tip of the corrosion wire exceeds the fracture toughness of the material, the crack would be unstable to cause the wire broken. However, the crack tip stress intensity factor K_I is as follows

$$K_I = \sigma \sqrt{\pi a} F(a/d_{\min}) \quad (11)$$

where σ is the average stress of the net cross section of corrosion wire; $F(a/d_{\min})$ is the function related to the shape of the crack which is as follows for the tension bar with semicircular cracks (Mahmoud 2007)

$$F(a/d_{\min}) = 0.7037 - 1.0589(a/d_{\min}) + 5.8771(a/d_{\min})^2 \quad (12)$$

Let K_{IC} be the fracture toughness of the material, as 67.5MPa \sqrt{m} for the steel wire, and K_{IB} the stress intensity factor for Type I crack. The fracture criteria $K_r = K_{IB}/K_{IC}$ is approximately the function of L_r , $L_r = \sigma/\sigma_y$, the ratio of σ and the yield stress of the material σ_y as follows

$$K_r = (1 - 0.14L_r^2) [0.3 + 0.7 \exp(-0.65L_r^6)] \quad (13)$$

It is obvious that the wire would be broken when $K_I/K_{IC} \leq K_r$.

However, the ultimate strength of the corrosion wire σ_c is as follows

$$\sigma_c = \frac{K_r K_{IC}}{\sqrt{\pi a} F(a_r/d)} \quad (14)$$

The cable can be regarded as a parallel system of wires. The corrosion and rupture of wires would result in the loss of net area of cross section of cable as well as its bear capacity. Therefore, the time-dependent cable strength under the coupling of corrosion and fatigue cracking can be estimated by the following steps:

Step 1. According to the corrosion model of the cable wires, Eq. (5) & Eq. (7), to estimate the cracking depth of the wire $a_i(t)$ near the damaged sheath;

Step 2. Base on the distribution model of the cross section of the cable, and the assumption of the unilateral

Type I cracking of the corrosion wire, to predict the equivalent corrosion depth $a_i(t)$, $i=1 \sim n$, n the total number of the wires of the cable, by using Eqs. (9) - (10);

Step 3. By using Eq. (11) and Eq. (14) to get the ultimate stress intensity factor K_{II} and the ultimate strength σ_{c_i} for each wire of the cable respectively;

Step 4. Sum up all the ultimate strength σ_{c_i} of the wires to obtain the ultimate strength of the cable at time t .

During the simulation of the strength degradation, the load stress σ are based on the load effects analysis due to the living load and dead load in the service life of the bridge discussed in the next section.

3. Load Effects of the Cables

In the present paper, the static linear response of the bridge subject to the living load and the dead load is concerned while the reduction of the net area of the cable cross section due to corrosion and cracking is taken into account. However, the degradation of Young's modulus of the material is ignored for its trivial variation.

Consider the most critical working condition of the bridge to the train load when two trains head towards each other at the middle of the bridge. The static tension force S_{vi} of cable due to the train load is simplified to be proportion to the train load F_v so that $S_{vi} = k_{vi} \cdot F_v$, where k_{vi} is the coefficient of the train load effect. The train load F_v follows the Gaussian distribution with the mean value 140, variance 14 and the coefficient of variation 0.1 for the train of type B1 running on the bridge (Cao 1995).

The wind effects on the bridge include two parts, namely the static effects due to the average wind speed and the dynamic effects due to the fluctuation wind speed. According to the design code of highway bridges in China (JTG/T 3360-01-2018 2018), the average design wind speed of the bridge is as follows

$$V_d = \bar{V}(10) \left(\frac{Z}{10} \right)^\alpha \quad (15)$$

where V_d and $\bar{V}(10)$ are the design wind speed for the reference height Z and the wind speed at 10m high above the ground, respectively. α is the surface roughness of the site, to be 0.16 herein. The mean wind speed of the girder of the simulated bridge is 38.6m/s.

For simplification, only the effect of horizontal fluctuating wind load is considered. The Davenport spectrum is used for the horizontal fluctuating wind as follows

$$S_v(\omega) = 4K\bar{V}^2(10) \frac{x}{\omega(1+x^2)^{4/3}} \quad (16)$$

where $x = 600\omega/\pi\bar{V}(10)$, K is taken as 0.005.

Assume the fluctuating wind process is the Gaussian stationary process with zero mean. The variance of the horizontal fluctuating wind speed is obtained by the integration of the spectra density function shown in Eq. (16). According to the statistics of wind data in Chongqing, the variance of the fluctuating wind speed for the simulated bridge is 4.589. Thus, the total wind speed V is the sum of the average wind speed and the

fluctuating wind speed and follows the Gaussian distribution function with the mean value 38.6 and the variance 4.589.

The wind pressures on the components of the bridge are as follows

$$F_w = \begin{cases} \frac{1}{2} \rho V^2 C_H H & \text{for girder} \\ \frac{1}{2} \rho V^2 C_H A_n & \text{for piers, tower and cables} \end{cases} \quad (17)$$

where, ρ is the air density, 1.25kg/m^3 , H is the height of the girder, C_H is the damping coefficient, as 1.67 herein.

A_n the area along the wind of the components of the bridge.

In the view of linear analysis, the tension force of cable due to wind load can be simplified as linear function of the square of wind speed V^2 , that is $S_{wi} = k_{wi} \cdot V^2, i=1 \sim n$, where k_{wi} is the force coefficient of cable to wind load.

Therefore, the total internal forces of the bridge cable are the sum of the effects of dead load, average and fluctuating wind load as follows

$$S_i = S_{vi}(t) + S_{wi}(t) + S_{Gi}(t) = k_{vi} \cdot F_v + k_{wi} \cdot V^2, \quad i=1 \sim n \quad (18)$$

where, the load coefficients k_{vi} and k_{wi} are varied with the deterioration of cables.

4. Degradation of the Back Cable Strength

A cable-stayed bridge with two towers and two cable planes in Chongqing was selected for numerical example. The overall length of the bridge is 640m with the facade shown in Fig.2., and height of the tower is 179.5m. The net width of the bridge deck is 14.5m and the interval space between the stay cables is 8m. The main girder is the prestressed concrete box with single-box and single-chamber that is 14.5m wide and 3.5m high. By using the software ANSYS, the finite element model was set for the time-varying strength analysis of cables to the interaction of corrosion and stress in service life. In the analysis, the beam element was used for girder and tower, and the rod element for cables. The cables are numbered from left to right as shown in Fig. 2. The information of the cable is shown in Table 1. The Diameter of the steel wire of the cable is 6mm with Elastic Modulus is 2.1×10^5 MPa and yield stress, 1860MPa.

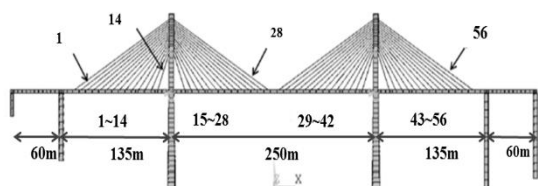


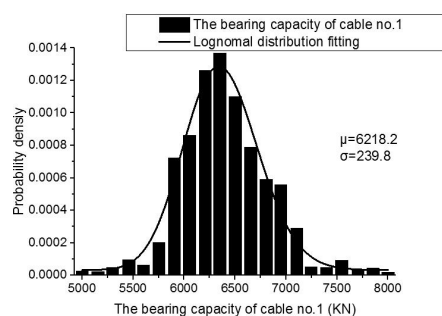
Figure 2. Facade and the FEM grids of the bridge.

Table 1. Information of the cable.

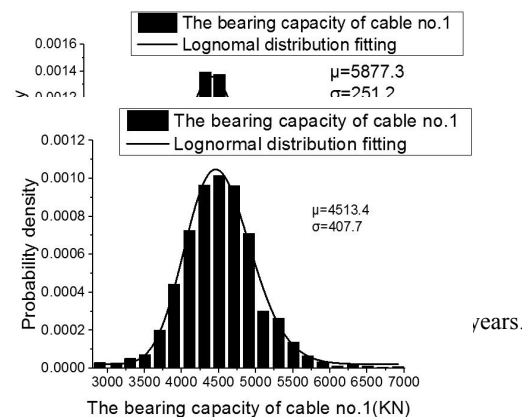
Cable Numbers	Amount of Wires	Cross-section of Cable (m ²)
1-4; 25-32; 53-56	258	0.0085
5-8; 21-24; 33-36; 49-52	222	0.0073
9-20; 37-48	186	0.0061

1-4; 25-32; 53-56	258	0.0085
5-8; 21-24; 33-36; 49-52	222	0.0073
9-20; 37-48	186	0.0061

Assume all the cables of the bridge in the uniform corrosion by ignoring the variation of the pitting corrosion and fatigue cracking for different cables with time and regarding all the coefficients of the corrosion models as constants. Combining the corrosion and the cracking due to the load stress, the degradation of the cable strengths are analyzed in which the distribution of the strength of the uncorroded wires are assumed as lognormal with mean value 1860MPa and the variance 0.16 and the uncertainty of the living load are taken into account as discussed in Sect.3.



(a) The bearing capacity distribution after 5 years



(c) The bearing capacity distribution after 20 year.

Figure 3. Bearing Capacity of Cable No.1 with time

Considering the strength and reliability of the back cable are dominant for the safety of the bridge, the back cable No.1 is selected for the bearing capacity degradation analysis. By using Monte-Carlo simulation method, 5000 samples of the bearing capacity of the

cable are simulated by the combination of the corrosion and cracking model as well as the load effects model, the distribution of the bearing capacities of Cable No.1 in 5, 10 and 20 years are shown in Fig. 3. It can be seen that, considering the uncertainty effects of corrosion and fatigue, the distribution function of the strength of Cable No.1 follows lognormal distribution. According to Fig. 4, it is shown that the mean value of the cable strength is decreased with time while the variance is increased, and both of the curves are getting steep with time. After 20 years, the mean value of the strength of Cable No.1 reduced to 72% of that at 5 year and the variance is about 1.7 times of that at 5 year approximately. The decrease of the mean value with the increase of the variance of the strength of the back cable is critical for the reliability of the bridge.

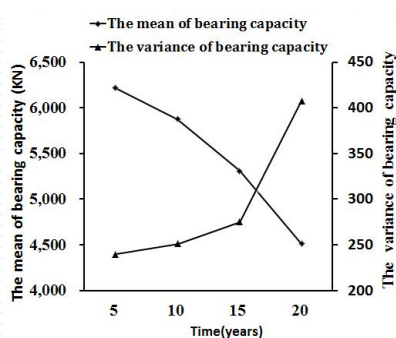


Figure 4. The mean value and variance of strength of Cable No.1 with time.

5. Reliability Analysis of Cable to coupling effects of Corrosion and Fatigue

However, the performance function of cable can be expressed as

$$g_i = R_i(t) - k_{vi}(t) \cdot F_v - k_{wi}(t) \cdot V^2 - S_{Gi}(t), i=1 \sim n \quad (19)$$

where the cable bearing capacities $R_i(t)$ are random variables that follow the lognormal distribution with the mean values decreased and the variances increased with time as discussed in Sec.2 due to the effects of corrosion and stress. The living load such as the train load and the wind load are regarded as random variables also that follow the normal distribution. The load effects coefficients are also varied with time due to the reducing of the cable net cross section. The dead load effect $S_{Gi}(t)$ is regarded as constant.

In order to investigate the time variation of the bearing capacities and the reliabilities of different cables, the back cable No. 1 and No. 56, the long cable at the middle of the bridge, No. 28 and the short cable near the tower, No.14 were analyzed. The bear capacities and the reliability indexes of cables are shown in Fig. 5 and 6 respectively. It is shown that, with the service time, the bearing capacities as well as the reliability indexes of these cables degraded rapidly. The strengths of the back cables are larger than the others, while the strength of the short cable near the tower, No.14 is the smallest. However, although the strengths of cables are quite different, the reliabilities of them are close, especially the

reliabilities of the two back cables coincided with each other very well.

According to Fig. 5 and 6, the time varying curves of the strengths as well as the reliability indexes also showed that in the early age of service life, see less than 10 years, the degradation rates of these curves are quite the same. After 10 years, the degradation rates became different. The degradations rate of the strength and the reliability index of the short cable 14 are slower than others. After 15 years, the strengths and the reliability indexes of the long cable No.28 decreased more rapidly than others. After 20 years, the reliability index of the back cables reduced to 3.975 that is around 1/4 of the original value in the beginning of the service life.

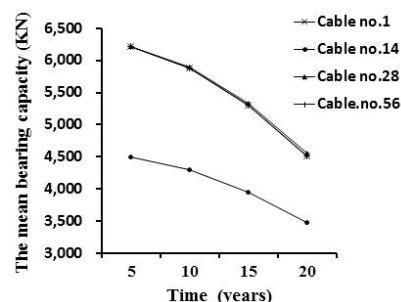


Figure 5. Mean values of bearing capacities of cables with time.

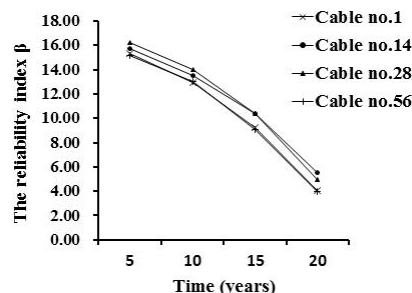
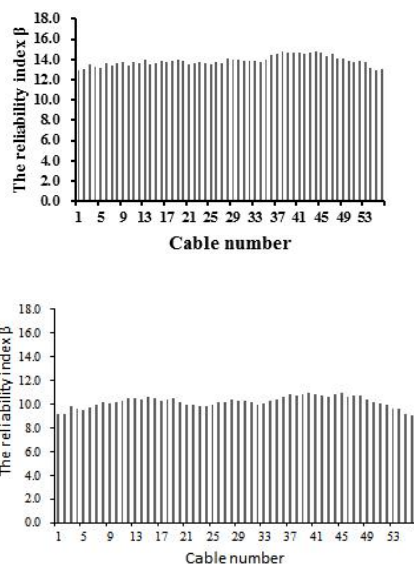


Figure 6. Reliability indexes of the cables with time.

The aforementioned degradation trends of the strength and the reliability of cables are caused by the interaction between corrosion and fatigue stress of the bridge during the service life. In the beginning of service life, the cables kept in good condition with high bearing capacities and reliabilities. With the pitting corrosion caused by the aging of HDPE and the erosion of the zinc coat of cables, the bearing capacities and reliabilities of cables degraded obviously because of the reducing of the net cross sections of corrosion cables. Further, due to the different stresses of the cables, the degradation rate of the bearing capacities of cables are different. The larger the stresses of the cables, the faster the degradation evolved. Therefore, the strength of the back cables No.1 and 56 are suffered much more severe to the corrosion and fatigue stress in the late age of service life than the others, especially than the short cable near the tower that subjected to lower stress.

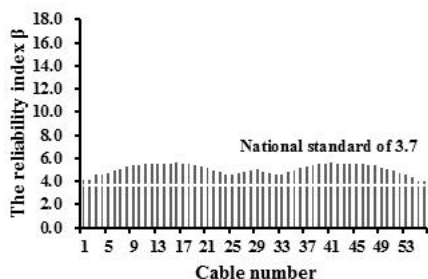
In Fig. 7, the prediction of the reliability indexes of all cables of the bridge with service time are given. It is shown that, the reliabilities of all the cables of the bridge

are in the same level in the early age of the service life, before 10 years of the service life. After 15 years, the reliabilities of the cables decreased and the differences between cables are shown. The reliabilities of the back cables and the long cables at the middle of the bridge are smaller than those near the tower. After 20 years, the reliability of all the cables decreased dramatically.



(a) Reliability index distribution of cables after 10 years.

(b) Reliability index distribution of stay cables after 15 years



(c) Reliability index distribution of cables after 20 years.

Figure 7. Reliable indexes of cables of the cable-stayed bridges.

6. Conclusions

Based on the corrosion and fatigue mechanism of cable wires, the degradation of the strengths and the reliabilities of cables for cable-stayed bridge in natural environment are analyzed. The main results are as follows:

(1) The variation of the cable strength with time: Under the interaction of corrosion and stress, the cable strength deduced with time and their distribution follows the lognormal distribution with the mean value decreases and the variances increase with time. The degradation rate of the cable strengths became rapidly at the late age of the service life of the bridge.

(2) The stresses of the cables subjected to the living load and dead load of the bridge have great effects on the degradation of cable strength. Based on the uniform corrosion assumption between cables, the larger the load stresses are, the more severe the cable strengths degrade

with time, such as the strengths of the back cables and the long cables of the bridge.

(3) In the early age of the service life of the bridge, the reliabilities of all the cables are in the same level. After 15 years, the reliabilities of the cables decreased and the differences between cables are shown. The reliabilities of the back cables and the long cables at the middle of the bridge that have larger stress are smaller than those near the tower. After 20 years, the reliability of all the cables decreased dramatically.

In the present work, the assumption of the uniform corrosion for all the cables with the constant expansion rate of the pitting corrosion at the cross section of the cable may overestimate the corrosion phenomena of the cable-stayed bridge. However, the time-varying cable strength and reliability and the effects of the load stress on the degradation of the cable strength showed in the present work are beneficial for the maintenance of cable-stayed bridge.

References

- Bruneau, M. 1992. Evaluation of system-reliability methods for cable-stayed bridge design. *Journal of Structural Engineering*, 118(4): 1106–1120.
- Cao, Q.F. 1995. Discussion on Chinese railway train load standards from probability design method (I). *Railway Standard Design*, 2: 4-8.
- Chen, M.X. 2006. Development and prospect of cable-stayed bridges. *Chinese and Foreign Highway*, 26 (4): 76-86.
- JTG/T 3360-01-2018. 2018. *Wind-resistant Design Specification for Highway Bridge*. People's Communications Press, Beijing.
- Ebara, R. 2007. Corrosion fatigue crack initiation in 12% Cr stainless steel. *Materials Science & Engineering A*, (468-470): 109-113.
- Furuya, K., Kitagawa, M., Nakamura, S.I., et al. 2000. Corrosion mechanism and protection methods for suspension bridge cables. *Structural Engineering International*, 10(3): 189-193.
- Hopwood, T. and Havens, J.H. 1984. Inspection, prevention, and remedy of suspension bridge cable corrosion problems. *Inspection*.
- Li, W., Yan, Q.S. and Wang, Y. 2010. Reliability analysis of cable-stayed bridge system. *Journal of Shenyang University of Technology*, 2: 235-240.
- Li, Z., Lu, J.Z. and Ge, S. 2004. A probabilistic model for predicting corrosion fatigue life of eroded pits. *Mechanical Strength*, 26(s1): 226-228.
- Llorca, J. and Sanchez-Galvez, V. 1987. Fatigue threshold determination in high strength cold drawn eutectoid steel wires. *Journal of Chinese Society for Corrosion and protection*, 26(6): 869-882.
- Mahmoud, K.M. 2007. Fracture strength for a high strength steel bridge cable wire with a surface crack. *Theoretical & Applied Fracture Mechanics*, 48(2):152-160.
- Sriraman, M.R. and Pidaparti, R.M. 2010. Crack initiation life of materials under combined pitting corrosion and cyclic loading. *Journal of Materials*

Engineering and Performance, 19(1):7-12.

Wang, L.L. and Yi, W.T. 2007. Corrosion cases and analysis of stay cables. *Central South Highway Engineering*, 32 (1): 94-98.

Wang, R. 1998. Fracture model of corrosion fatigue crack growth. *Journal of Chinese Society for Corrosion and protection*, 18 (2): 87-94.

Xu, H., Huang, P.M. and Han, W.S. 2008. Analysis and evaluation of the strength and safety of parallel wire slings. *Journal of Safety and Environment*, 8(5): 122-125.

Xu, J. 2006. Damage evolution mechanism and remaining life evaluation of cable. *Ph.D Thesis*. Department of bridge and tunnel engineering, Shanghai.

Xu, K.J., Jiang, L.P. and Sui, Y.S. 2003. Probabilistic method for predicting corrosion fatigue life. *Mechanical Strength*, 25 (2): 229-232.